# Early Thermal Evolution of Planetesimals and its Impact on Processing and Dating of Meteoritic Material

H.-P. Gail [1] D. Breuer [2], T. Spohn [2], T. Kleine [3], M. Trieloff [4]

[1] Institute of Theoretical Astrophysics, Heidelberg University
[2] Institute for Planetary Research, DLR Berlin
[3] Institute of Planetology, Münster University
[4] Institute of Earth Sciences, Heidelberg University

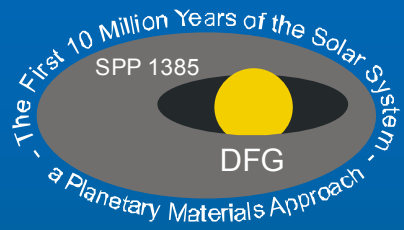

# Meteorites: Fragments of small bodies in the solar system, the asteroids between Mars and Jupiter

- Inferred number of parent bodies is ~100
- Accretion to full-sized planet inhibited by early Jupiter

Innisfree

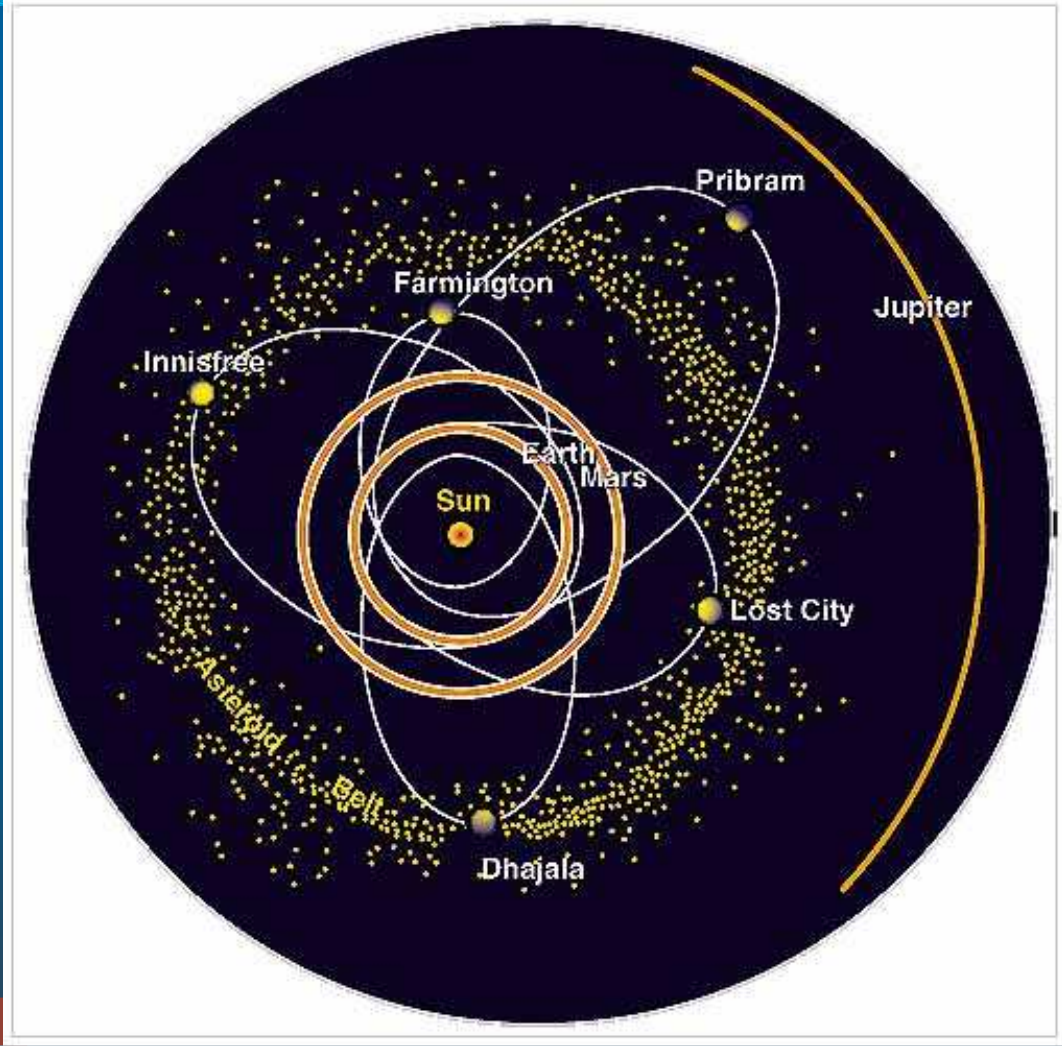

# Carbonaceous chondrites (mild thermal/aqueous metamorphism)

→undifferentiated, e.g. preaccretional structures preserved

- Chondrules → ~1400-1600 K
- Ca,Al-rich inclusions → ~1800-2000 K
- Fine grained matrix (volatile rich) <900 K

→undifferentiated, e.g. 'cosmic' Fe,Ni abundance

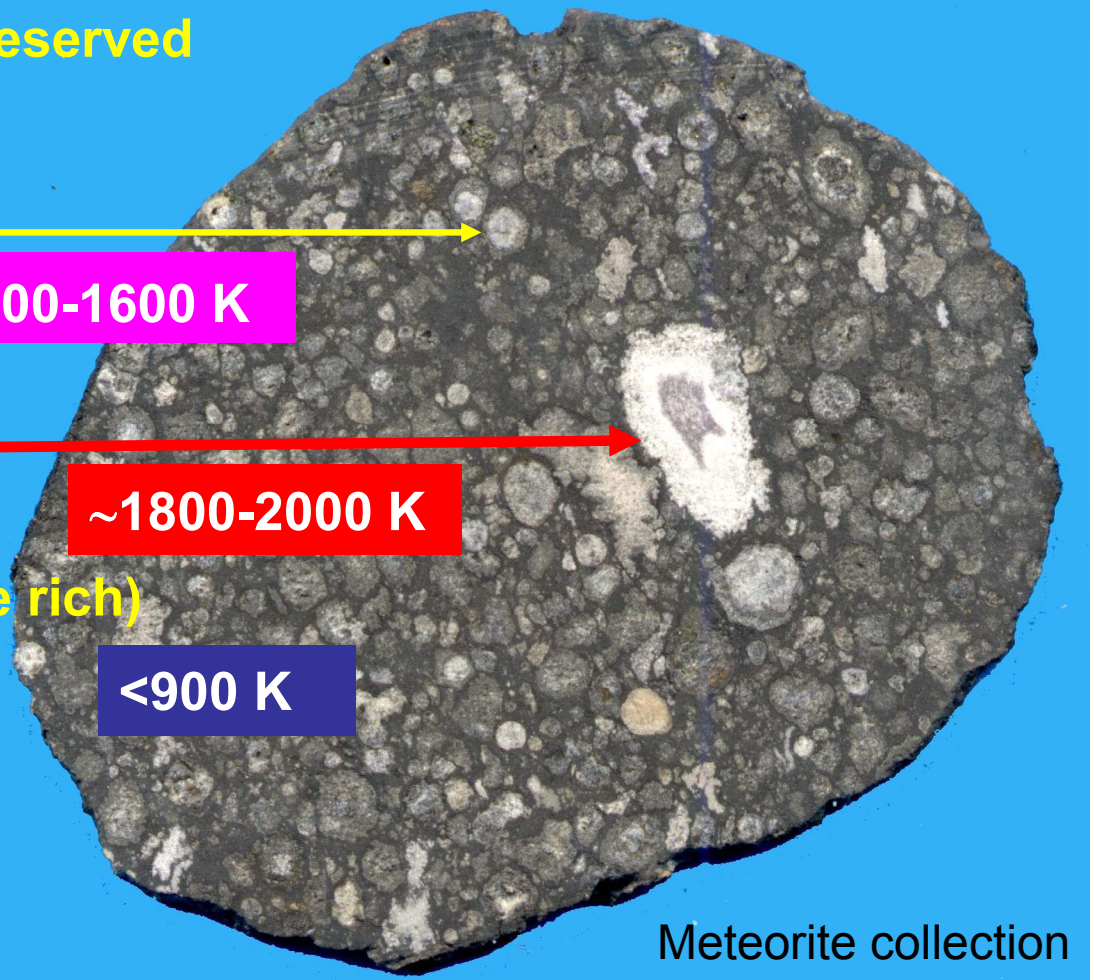

Meteorite collection
Dieter Heinlein, Augsburg, Germany

**4564.7± 0.6 Ma**
**(CR Acfer059;**
**Amelin et al., 2002)**

- **Chondrules**

- **Ca,Al-rich inclusions**

**4567.2± 0.6 Ma**
**(U-Pb-Pb, CV Efremovka;**
**Amelin et al., 2002)**

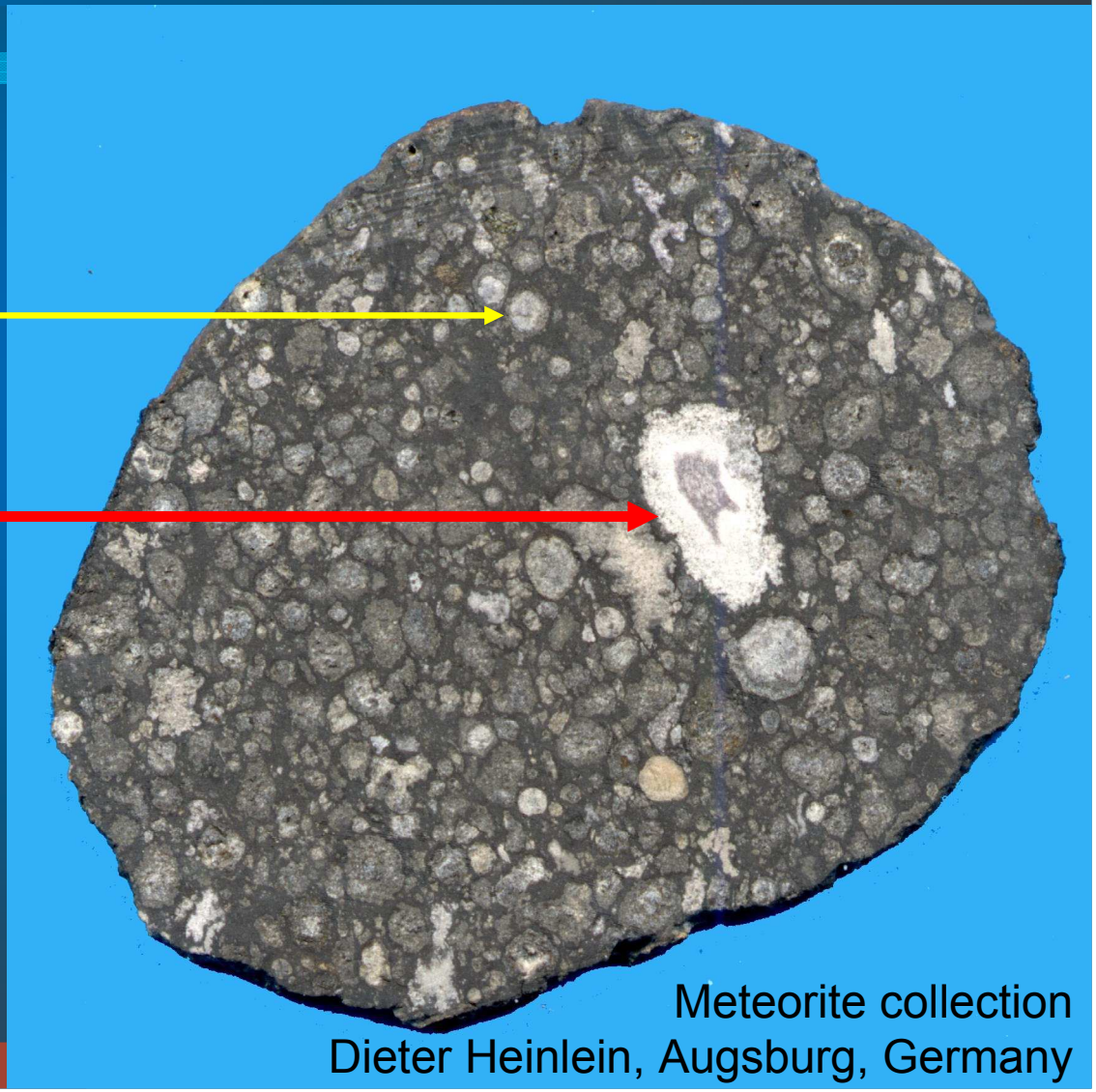

Meteorite collection
Dieter Heinlein, Augsburg, Germany

# Metal abundance of chondrites:
# Origin from primitive, undifferentiated parent bodies
# Variation of oxidation state and metal abundance:
# Origin from compositionally different parent asteroids

**Ordinary chondrites:**
**H: high Fe**
**L: Low Fe**
**LL: Low total, low metallic Fe**

**Enstatite chondrites**

**Carbonaceous chondrites:**
**named after main member**
**CI (Ivuna)**
**CM (Mighei)**
**CV (Vigarano)**
**CO (Ornans)**

Trieloff & Palme (2006) in: Planet Formation – Theory, Observations, and Experiments. Cambridge University Press

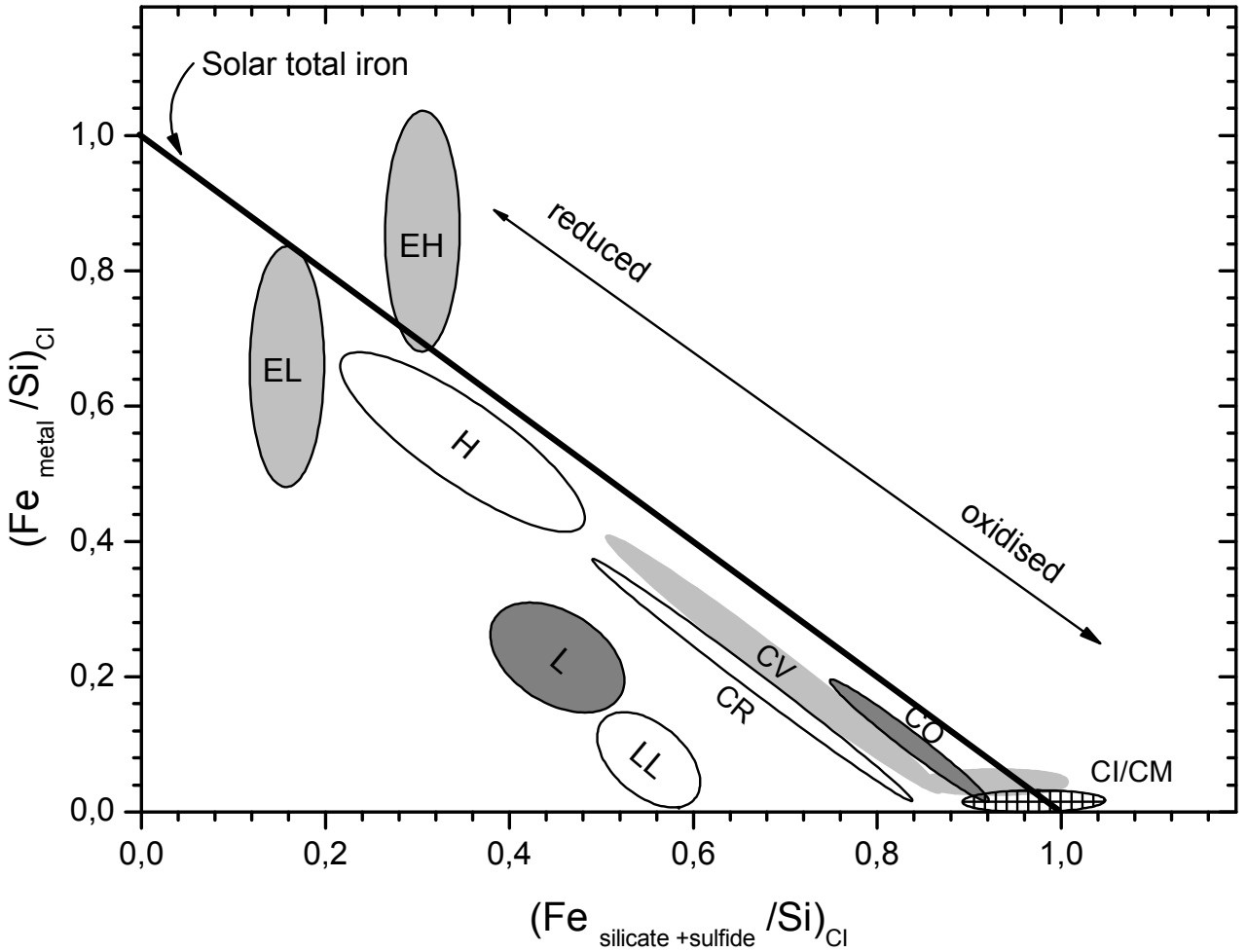

**Ca,Al-rich Inclusions: refractory mineral assemblages, oldest solar system objects → 4567.2± 0.6 Ma (Amelin et al., 2002)**
**→contain excess $^{26}$Mg from decay of short-lived $^{26}$Al**

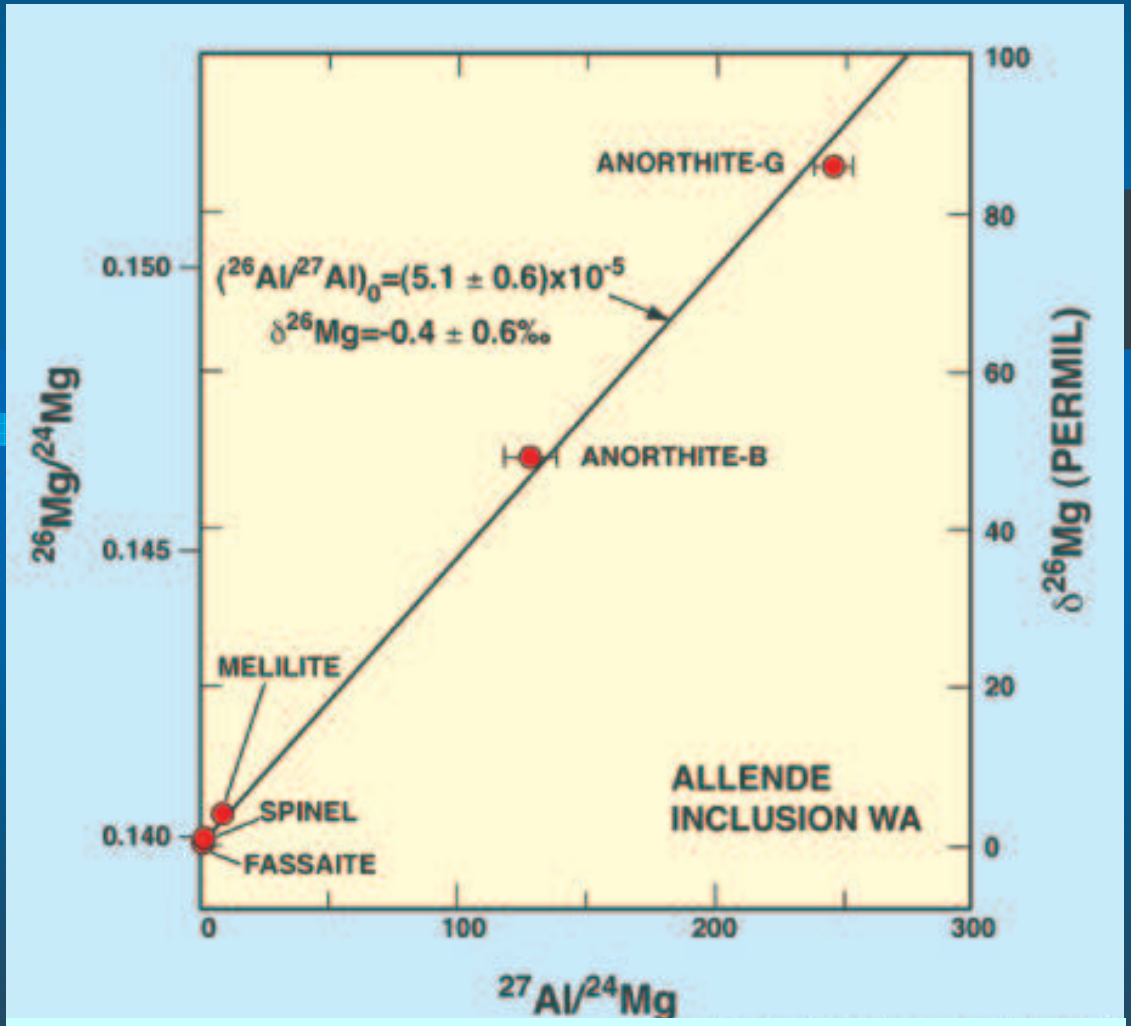


Lee et al. 1976 Geophys. Res. Lett. 3, 109

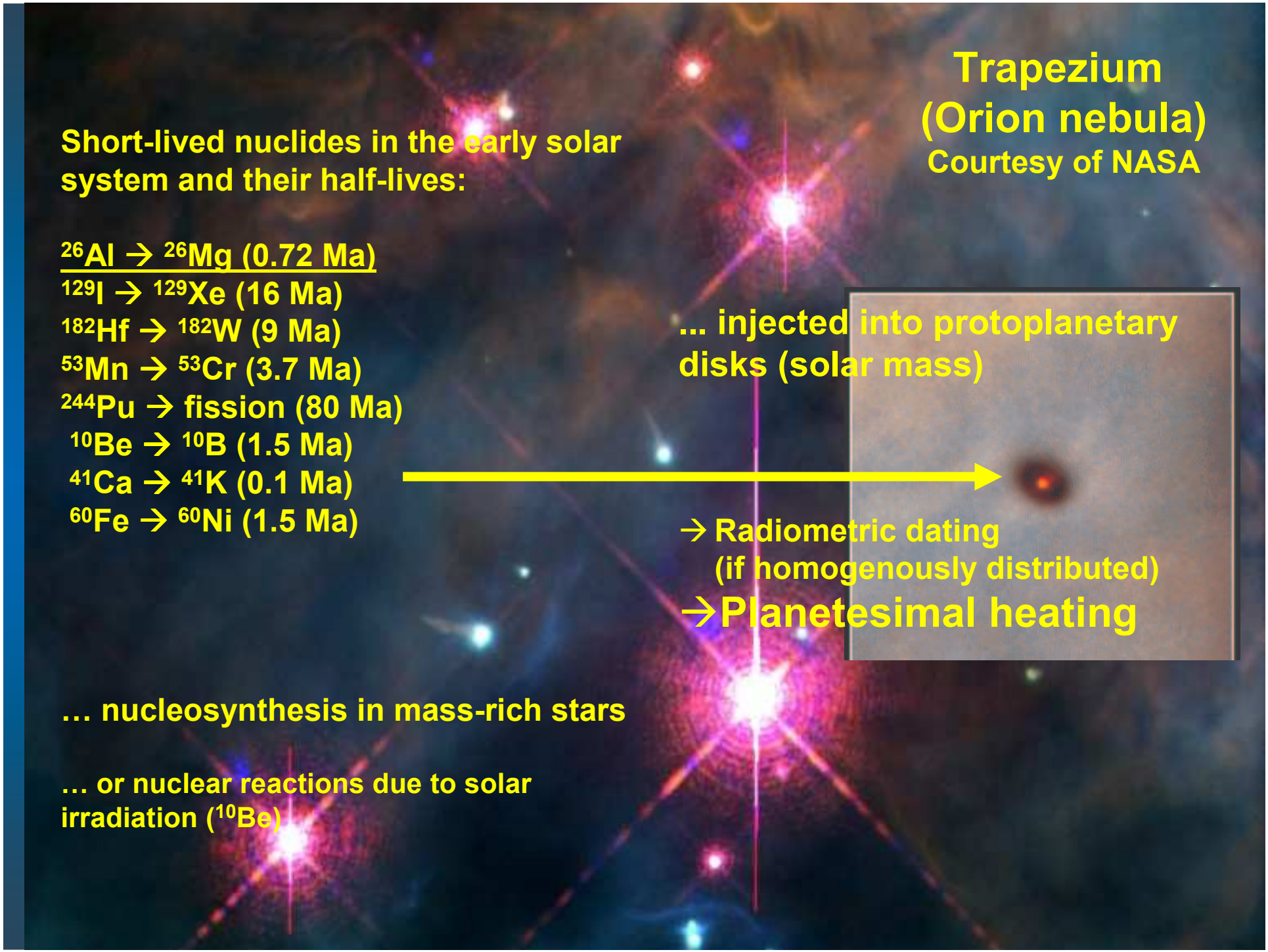
Trapezium
(Orion nebula)
Courtesy of NASA
Short-lived nuclides in the early solar system and their half-lives:
$^{26}Al \rightarrow {}^{26}Mg$ (0.72 Ma)
$^{129}I \rightarrow {}^{129}Xe$ (16 Ma)
$^{182}Hf \rightarrow {}^{182}W$ (9 Ma)
$^{53}Mn \rightarrow {}^{53}Cr$ (3.7 Ma)
$^{244}Pu \rightarrow$ fission (80 Ma)
$^{10}Be \rightarrow {}^{10}B$ (1.5 Ma)
$^{41}Ca \rightarrow {}^{41}K$ (0.1 Ma)
$^{60}Fe \rightarrow {}^{60}Ni$ (1.5 Ma)
... injected into protoplanetary disks (solar mass)
→ Radiometric dating
(if homogenously distributed)
→Planetesimal heating
… nucleosynthesis in mass-rich stars
… or nuclear reactions due to solar irradiation ($^{10}Be$)

## Formation of planetesimals and planets

→ growth from (sub)micrometer sized dust to km-sized planetesimals by hit- and-stick collisions

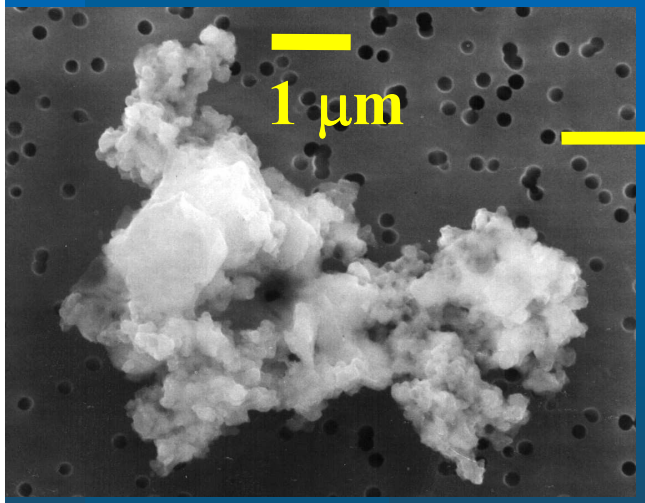


Courtesy of NASA

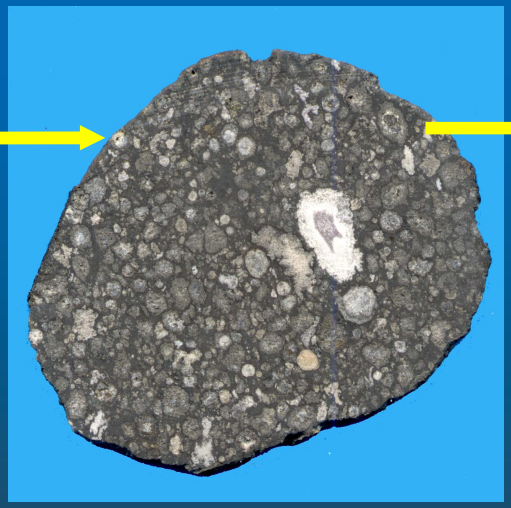

Meteorite collection Dieter Heinlein, Augsburg

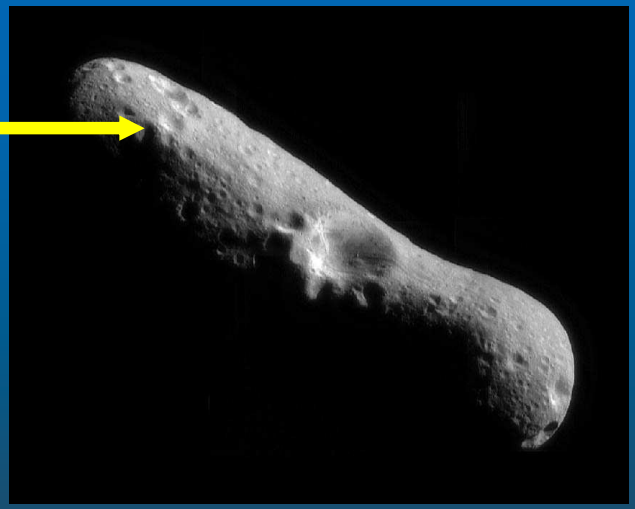

Courtesy of NASA

**Early formed asteroids: high abundance of $^{26}Al$, strongest heating effects → Differentiated meteorites: from metallic cores and silicate mantles and crusts of differentiated asteroids**

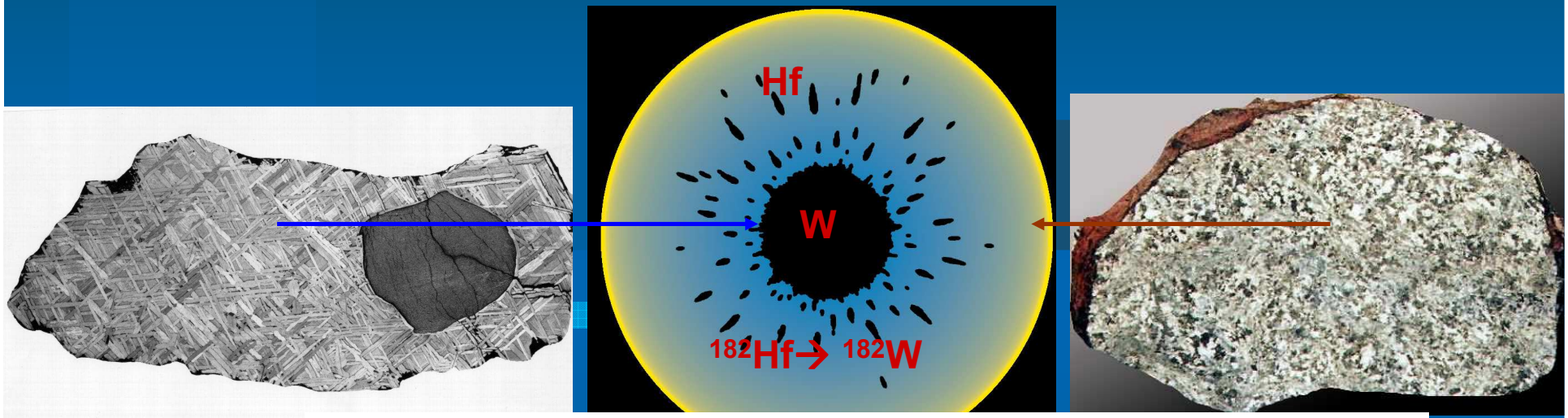


Trieloff & Althaus (2003) Sterne und Weltraum special 2, 83

**Fast accretion and differentiation**
**→formation of metallic cores contemporaneously with CAIs ($^{182}Hf$-$^{182}W$; Kleine et al., 2004; Schersten et al. 2004)**
**→formation and cooling of basaltic crust within few Ma (Eucrites, Angrites: Pb-Pb-dating; e.g. Lugmair and Galer, 1992; Baker et al.,. 2005)**

## $^{26}$Al as planetesimal heat source:
## Extent of heating as a function of $^{26}$Al content and accretion time after CAIs

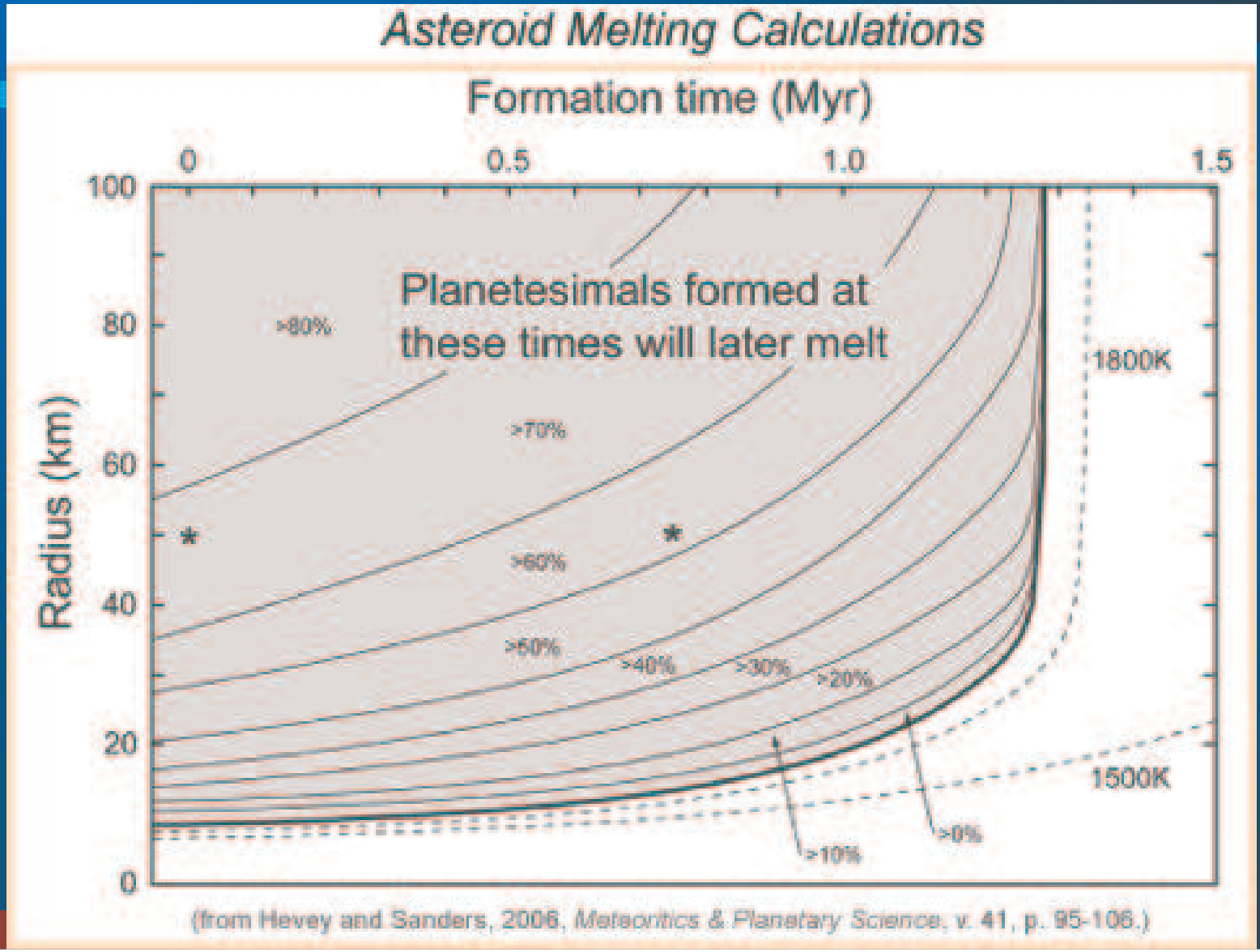

# Modeling the thermal evolution of small bodies

**Start with highly porous planetesimal with subsequent sintering**

**Implementation of porosity dependent heat conductivity of micrometer sized silicate aggregates**

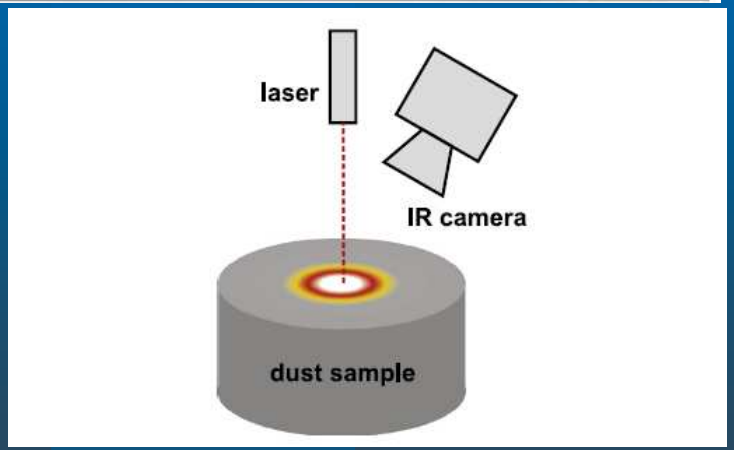


Krause et al. (2011) Icarus 214, 286

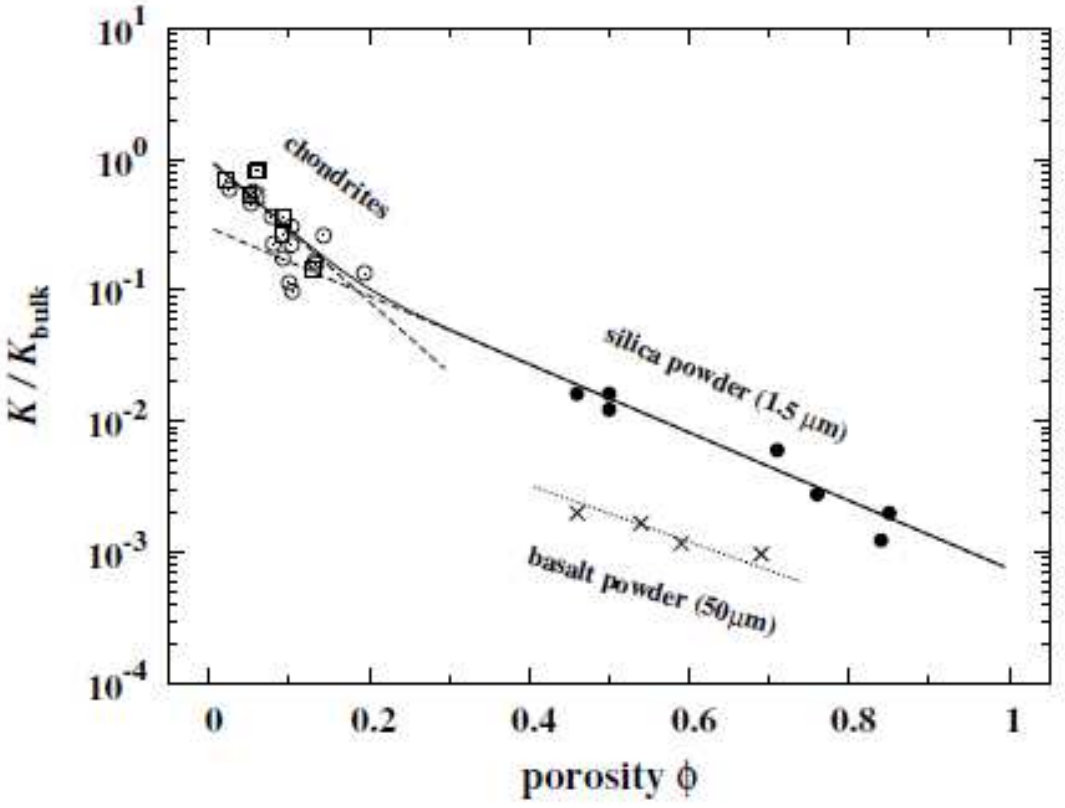

# Modeling the thermal evolution of small bodies

Start with highly porous planetesimal with subsequent sintering

Implementation of porosity dependent heat conductivity of micrometer sized silicate aggregates

Pressure and temperature stratification
→ equations of hydrostatic equilibrium and energy transport

Decrease of porosity of granular material by hot pressing due to self-gravity
→ set of equations for sintering of powder materials
(Kakar & Chaklader 1967, Rao & Chaklader 1972, Arzt et al. 1983, Yomogida & Matsui 1984)

$^{26}$Al and $^{60}$Fe heat sources (+long lived radioactivities) are taken into account

# Modeling the thermal evolution of small bodies

**Model starts with highly porous planetesimal with subsequent sintering**

**Decrease of porosity of granular material by hot pressing due to self-gravity**
**→set of equations for sintering of powder materials**
**(Kakar & Chaklader 1967, Rao & Chaklader 1972, Arzt et al. 1983, Yomogida & Matsui 1984)**

Henke et al. (2012) A&A 537, A45

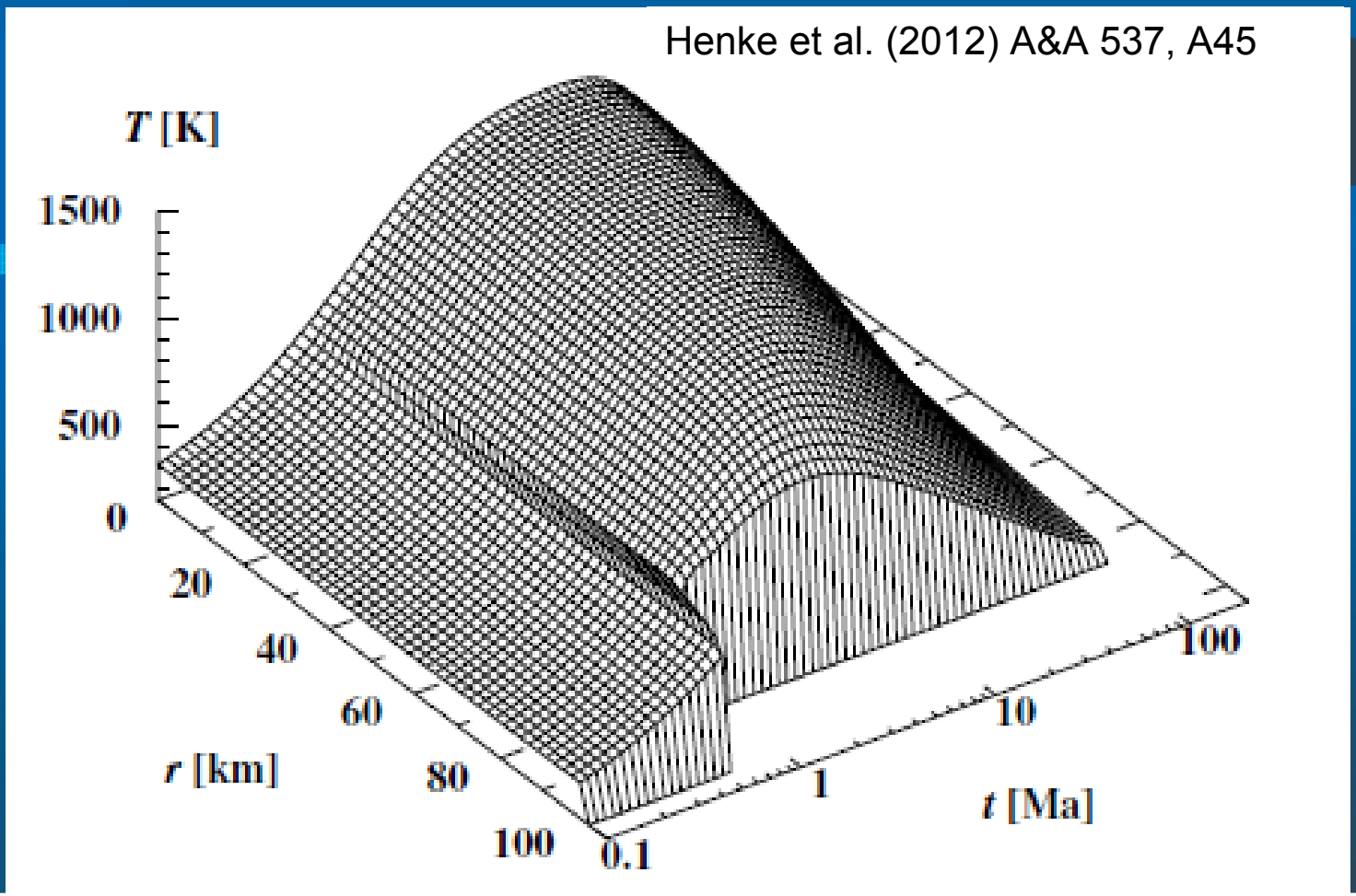

# Modeling the thermal evolution of small bodies

**Model starts with highly porous planetesimal with subsequent sintering**

**Decrease of porosity of granular material by hot pressing due to self-gravity**
**→set of equations for sintering of powder materials**
**(Kakar & Chaklader 1967, Rao & Chaklader 1972, Arzt et al. 1983, Yomogida & Matsui 1984)**

Henke et al. (2012) A&A 537, A45

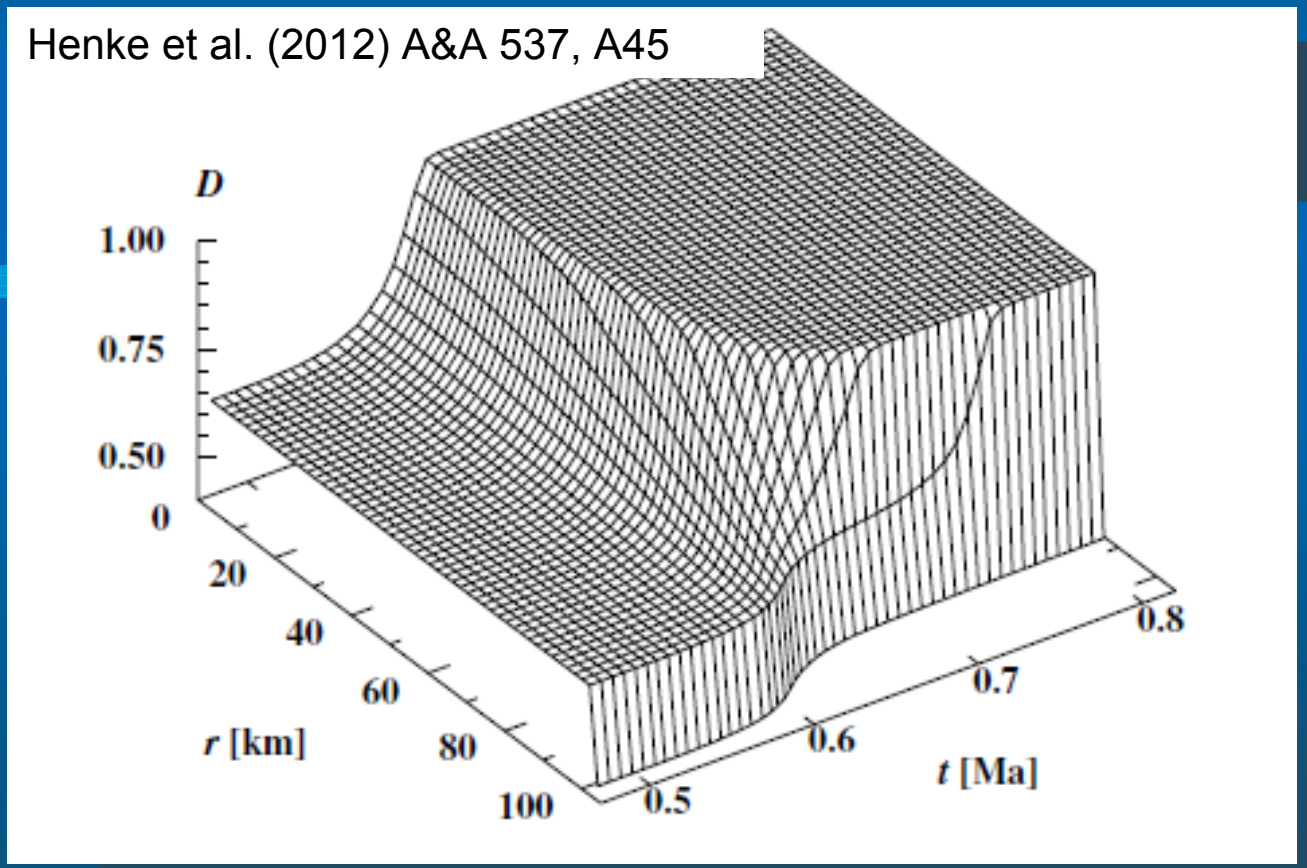

# Modeling the thermal evolution of small bodies

## Exploring the parameter space:
## Influence of porosity on heating of very small bodies
(instantaneous accretion)

Neumann et al. (2012) A&A 543, A141

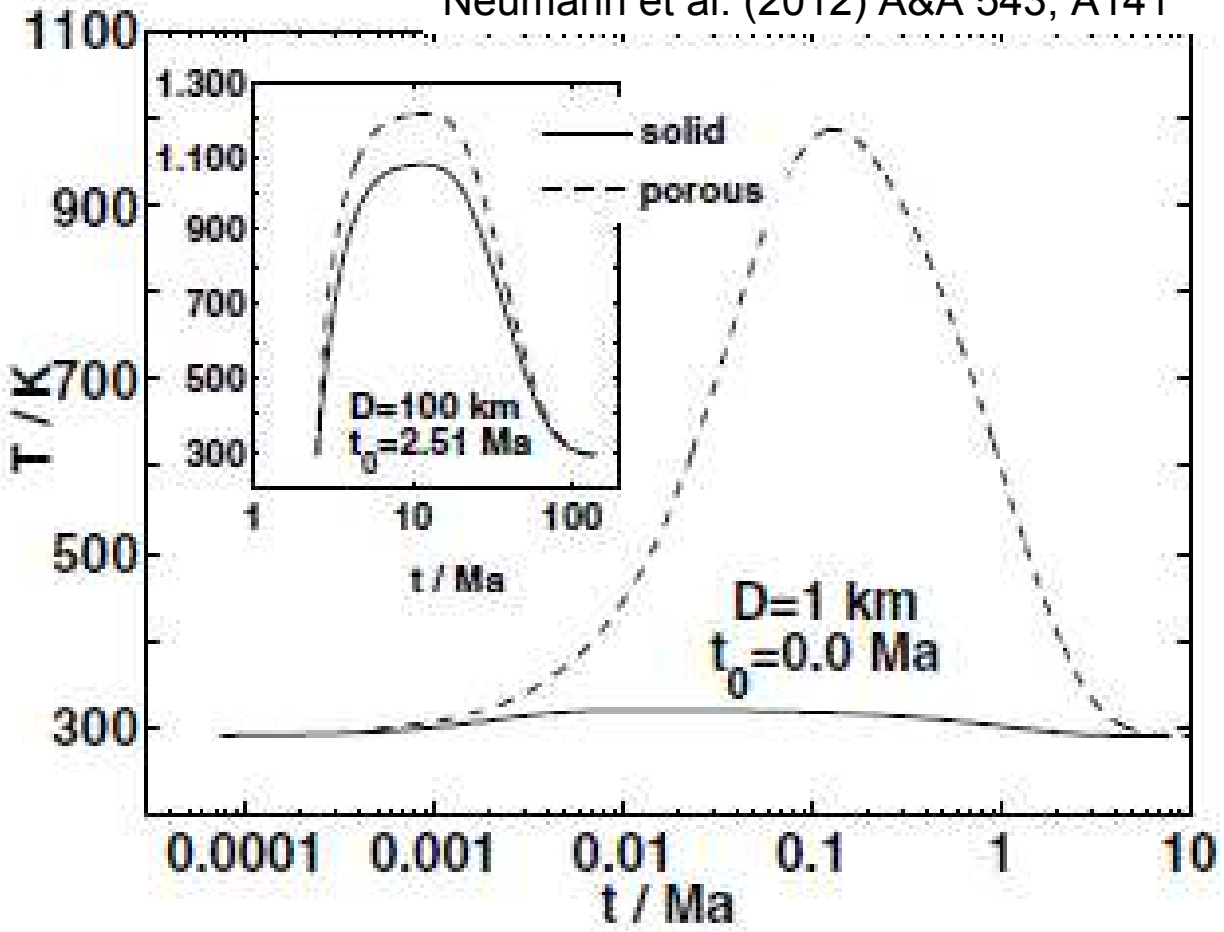

# Modeling the thermal evolution of small bodies

## Exploring the parameter space:
## Influence of duration of accretion
**(linear accretion to D=10km, 1.44 Ma after CAIs)**

Neumann et al. (2012) A&A 543, A141

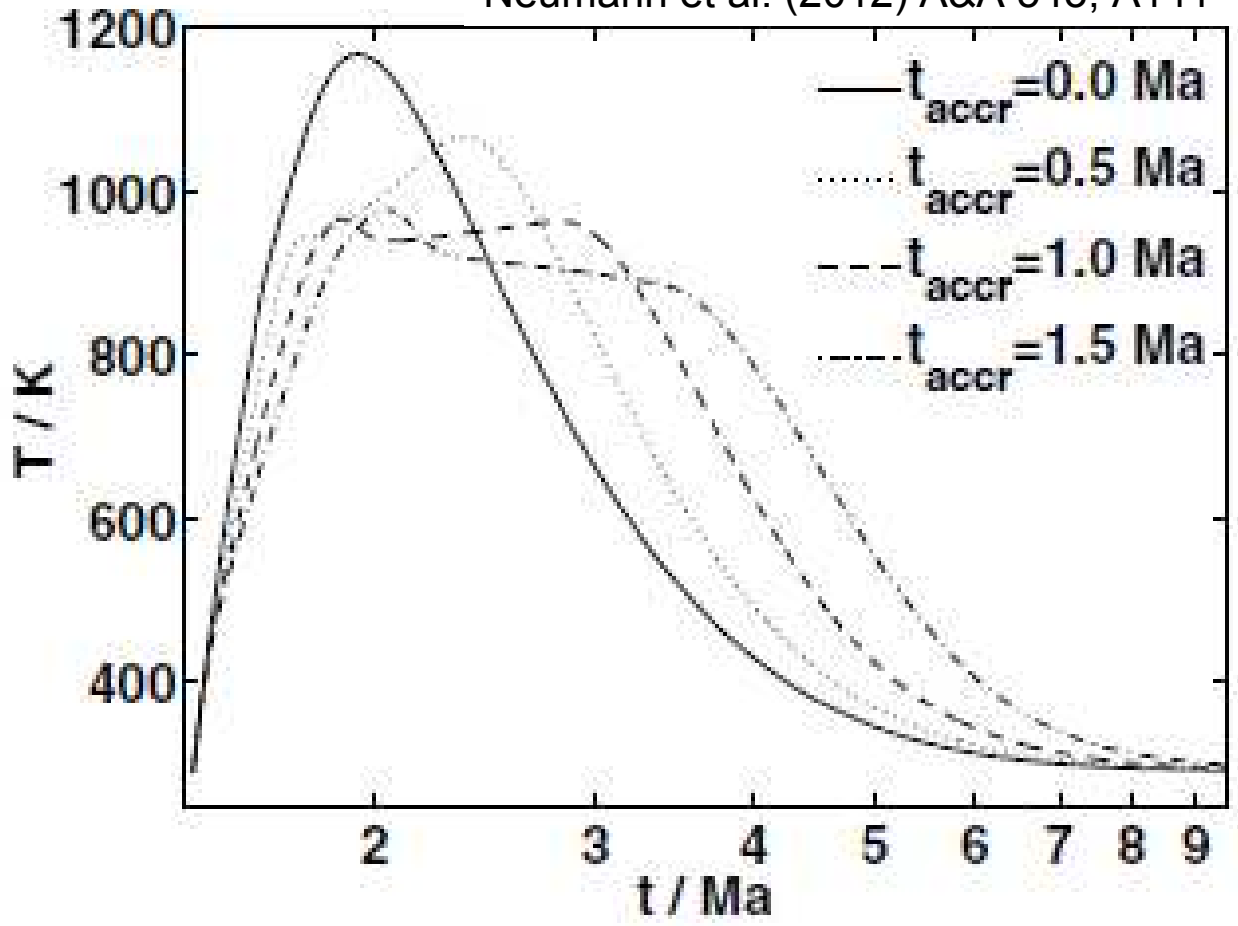

# Modeling the thermal evolution of small bodies

## Exploring the parameter space:
## Influence of accretion rate
**(accretion within 1 Ma to D=10km, 1.44 Ma after CAIs)**

Neumann et al. (2012) A&A 543, A141

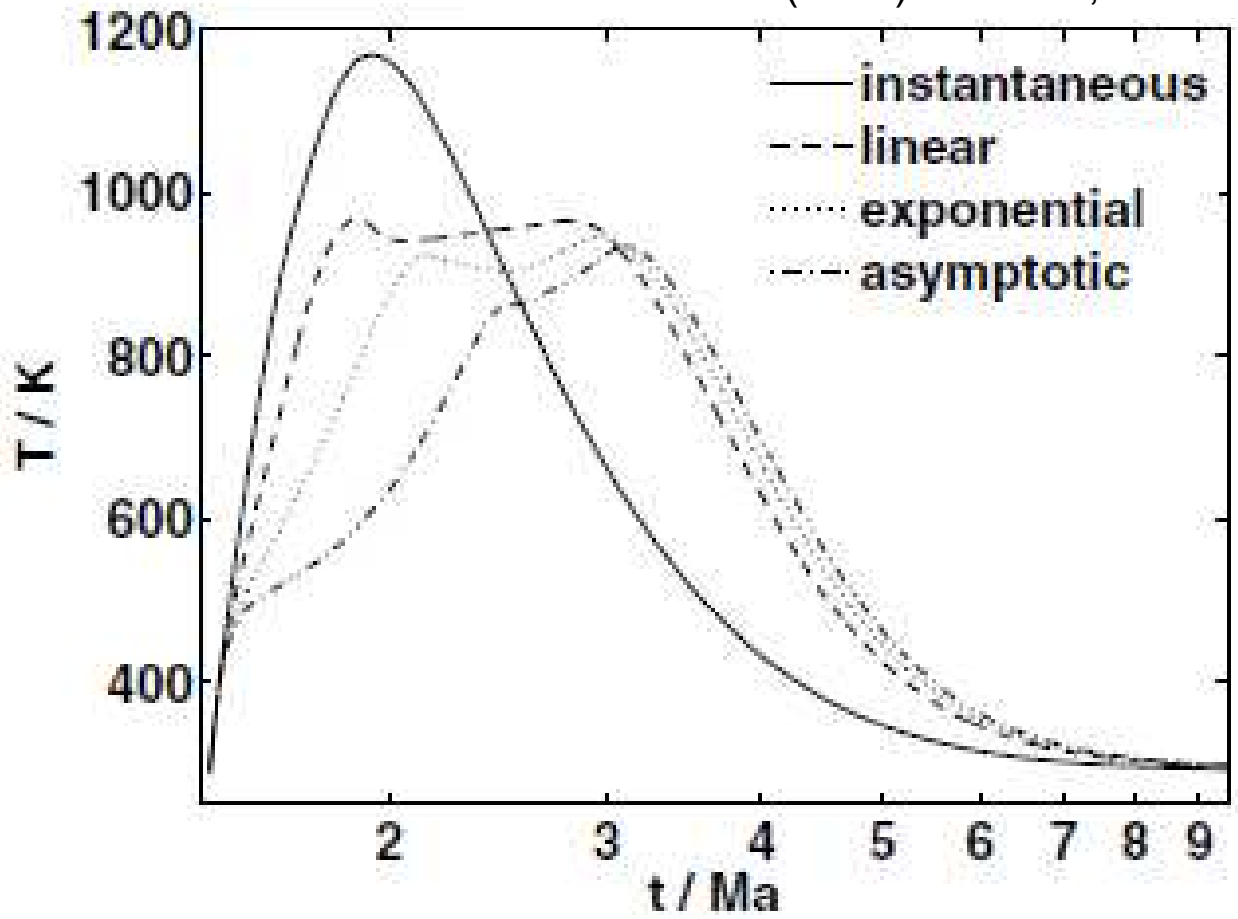

# Modeling the thermal evolution of small bodies

**Effect of porosity and $^{60}$Fe heating on central temperatures of bodies of different radius formed at different times (relative to CAIs)**

Henke et al. (2012) A&A 537, A45

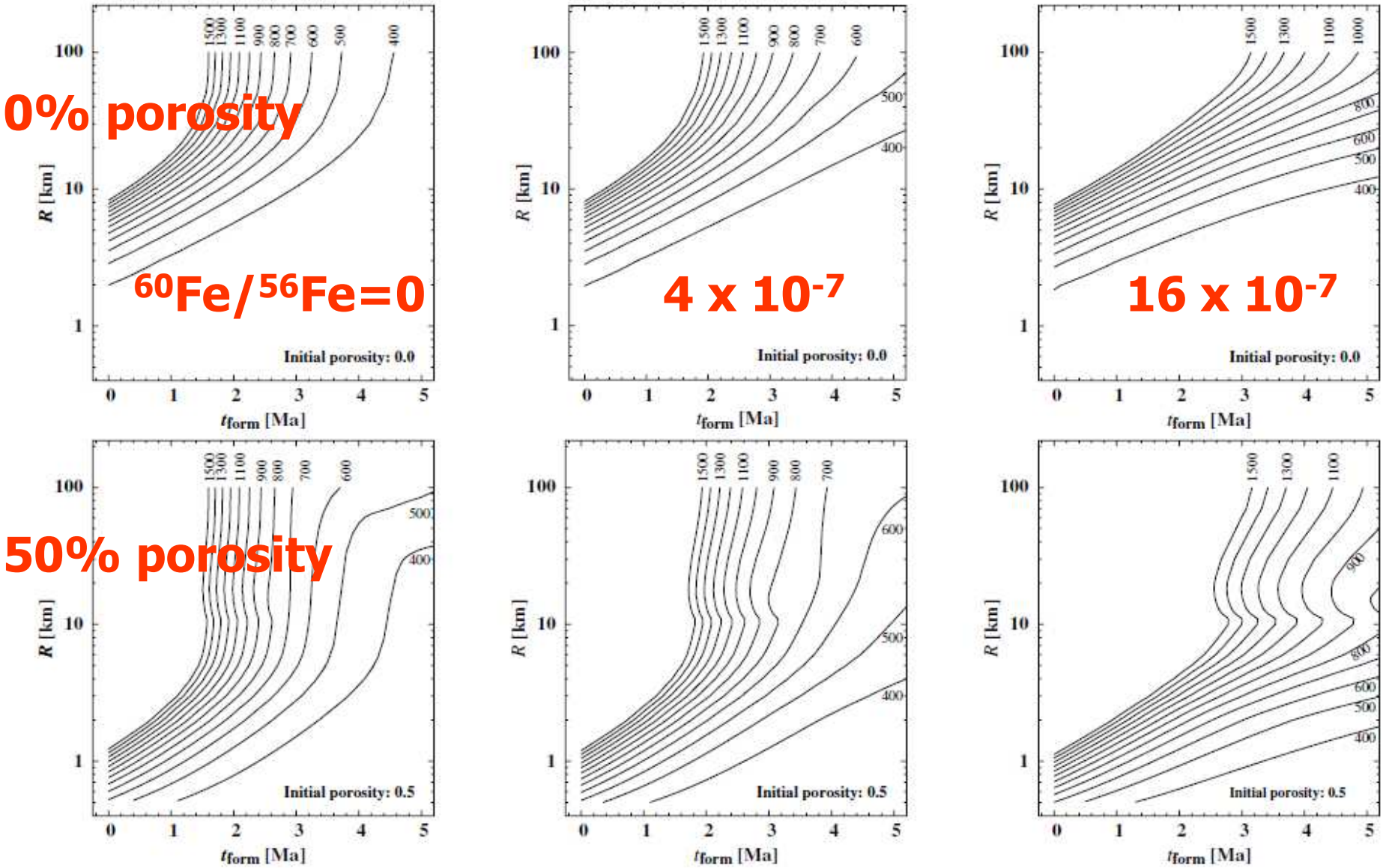

# Modeling the thermal evolution of small bodies

**Effect of porosity and $^{60}$Fe heating on central temperatures of bodies of different radius formed at different times (relative to CAIs)**

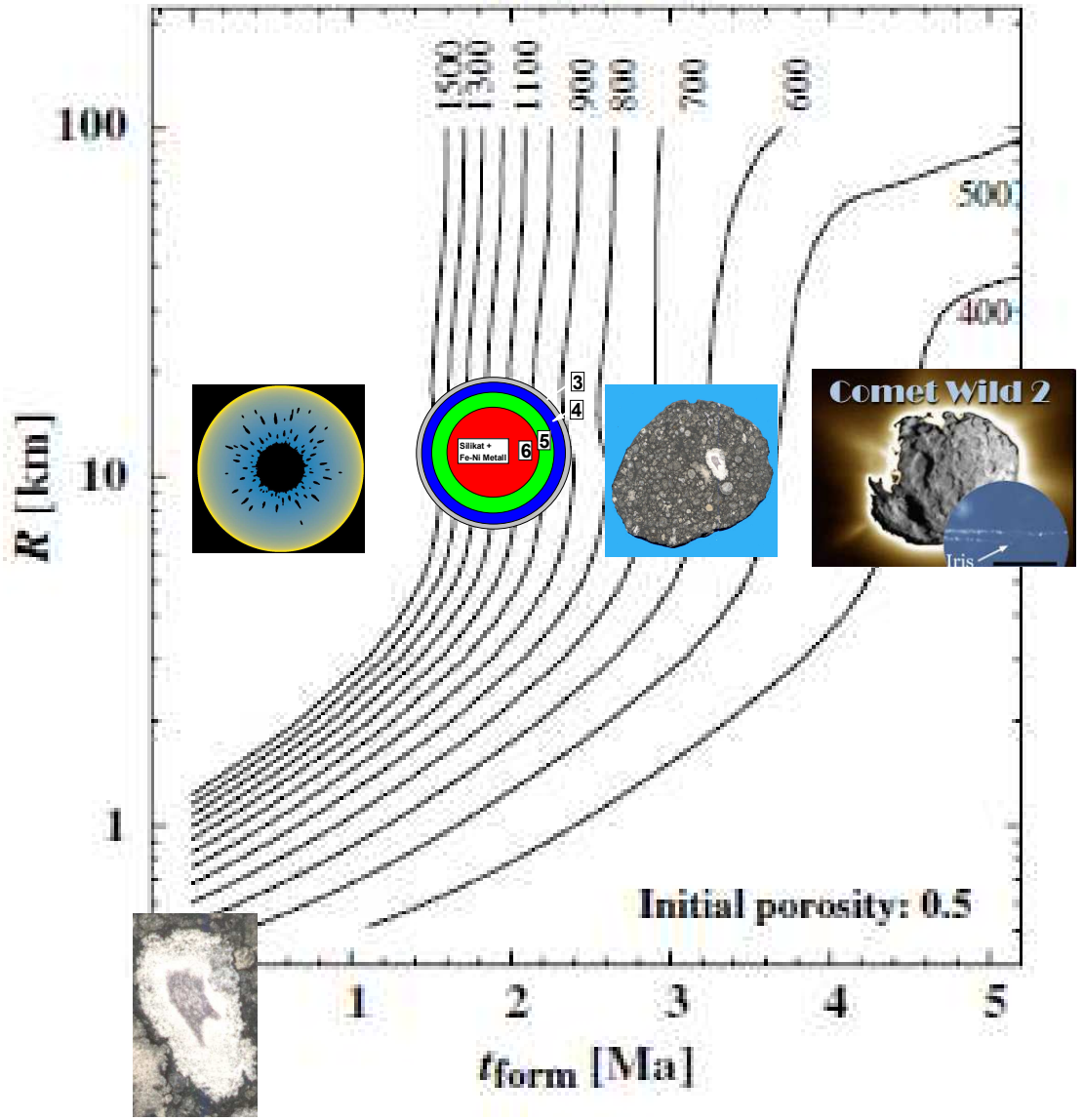

# Ordinary chondrites (H, L, LL): significant thermal metamorphism by $^{26}$Al decay heat

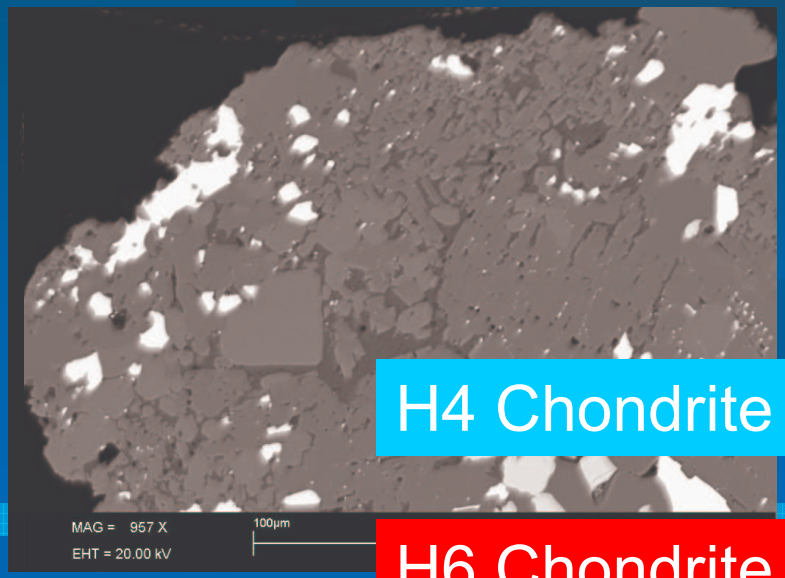


H4 Chondrite (~650°C)

H6 Chondrite (~850°C)

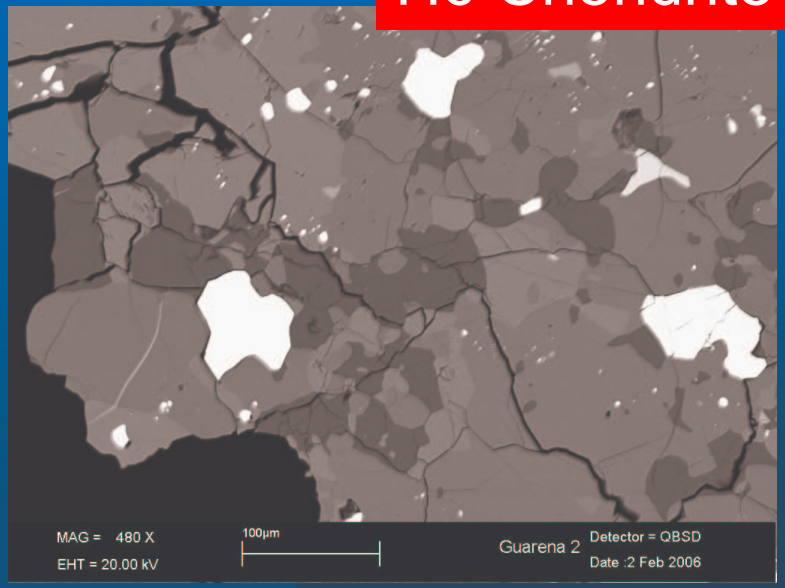


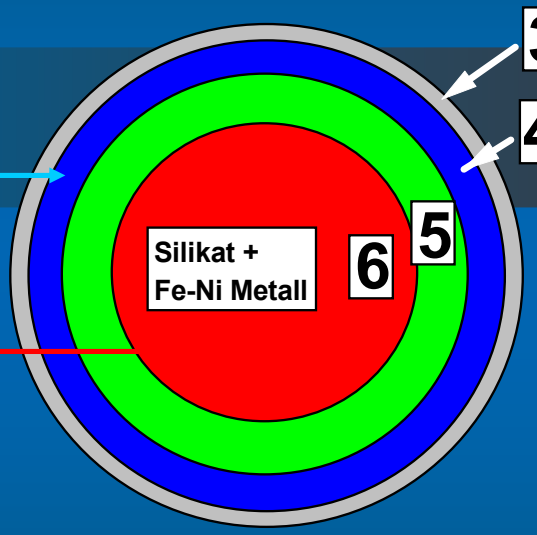

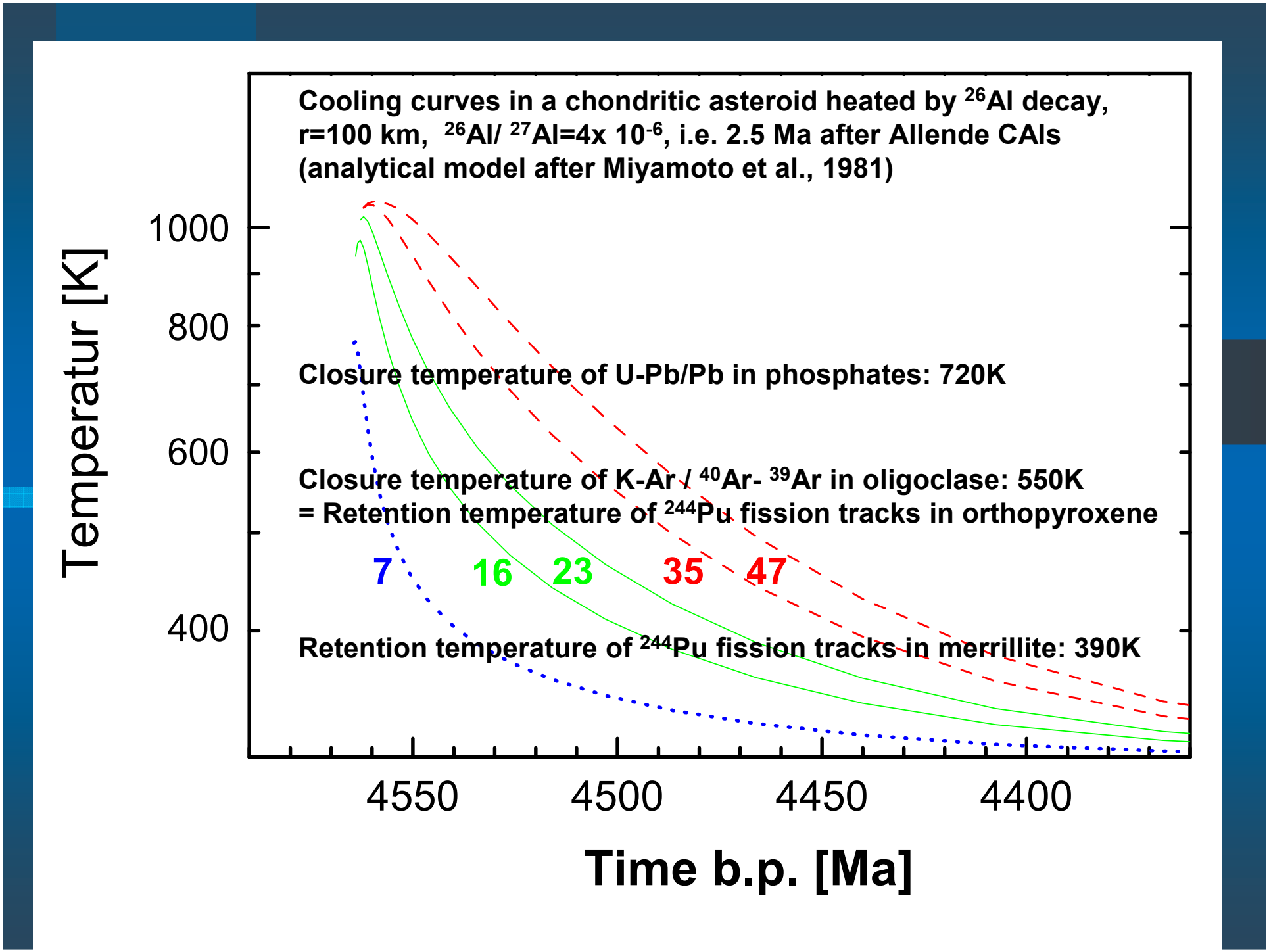
Cooling curves in a chondritic asteroid heated by 26Al decay,
r=100 km, 26Al/ 27Al=4x 10-6, i.e. 2.5 Ma after Allende CAIs
(analytical model after Miyamoto et al., 1981)
Temperatur [K]
1000
800
600
400
Closure temperature of U-Pb/Pb in phosphates: 720K
Closure temperature of K-Ar / 40Ar- 39Ar in oligoclase: 550K
= Retention temperature of 244Pu fission tracks in orthopyroxene
7
16
23
35
47
Retention temperature of 244Pu fission tracks in merrillite: 390K
4550
4500
4450
4400
Time b.p. [Ma]

letters to nature

# Structure and thermal history of the H-chondrite parent asteroid revealed by thermochronometry

Mario Trieloff*, Elmar K. Jessberger†, Ingrid Herrwerth‡, Jens Hopp*‡, Christine Fiéni§, Marianne Ghélis§, Michèle Bourot-Denise§ & Paul Pellas§||

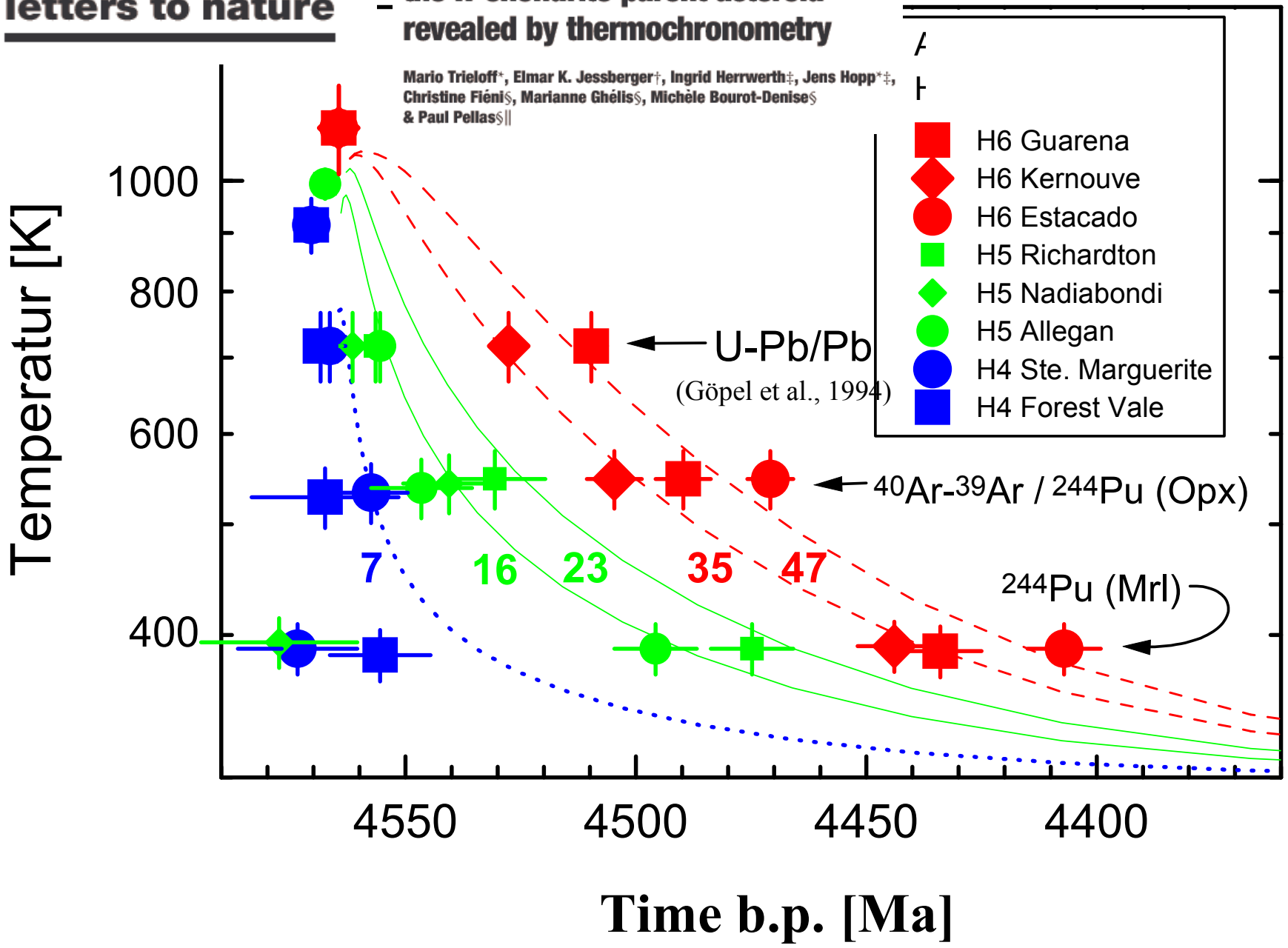

# Thermal model of the H chondrite parent body constrained by radioisotopic ages (Henke et al. 2012a,b, 2013)

Henke et al. (2013) Icarus 226, 212

Cooling ages of H-chondrites used in this study.

| Meteorite | Type | Hf–W[a] (metal-silicate) | Pb–Pb[b] (pyroxene olivine) | Al–Mg[c] (feldspar) | U–Pb–Pb[d] (phosphates) | Ar–Ar[e] (feldspar) | Pu-fission tracks[f] (merrillite) | |
|---|---|---|---|---|---|---|---|---|
| Closure temperature | | 1150 ± 75 (1100 ± 75 for Richardton) | 1050 ± 100 | 750 ± 130 | 720 ± 50 | 550 ± 20 | 390 ± 25 | K |
| Estacado | H6 | 4557.3 ± 1.6 | 4561 ± 7 | | 4501.6 ± 2.2 | 4465 ± 5 | 4401 ± 10 | Ma |
| Guareña | H6 | | | | 4504.4 ± 0.5 | 4458 ± 10 | 4402 ± 14 | Ma |
| Kernouvé | H6 | 4557.9 ± 1.0 | 4537.0 ± 1.1 | | 4522.5 ± 2.0 | 4499 ± 6 | 4438 ± 10 | Ma |
| Mt. Browne | H6 | | 4554.8 ± 6.3 | | 4543 ± 27 | 4516 ± 5 | 4471 ± 13 | Ma |
| Richardton | H5 | 4561.6 ± 0.8 | 4562.7 ± 1.7 | | 4551.4 ± 0.6 | 4525 ± 11 | 4469 ± 14 | Ma |
| Allegan | H5 | | | | 4550.2 ± 0.7 | 4541 ± 11 | 4490 ± 14 | Ma |
| Nadiabondi | H5 | | 4558.9 ± 2.3 | | 4555.6 ± 3.4 | 4535 ± 10 | 4543 ± 20 | Ma |
| Forest Vale | H4 | | | 4562.5 ± 0.2 | 4560.9 ± 0.7 | 4552 ± 8 | 4544 ± 14 | Ma |
| Ste. Marguerite | H4 | | | 4563.1 ± 0.2 | 4562.7 ± 0.6 | 4562 ± 16 | 4550 ± 17 | Ma |

**New data since 2003**

Notes:

[a] Hf–W ages are from Kleine et al. (2008) and were re-calculated relative to the $^{182}Hf/^{180}Hf$ of the angrite D'Orbigny, which has a Pb–Pb age of $t = 4563.4 \pm 0.3$ Ma (Kleine et al., 2012). Closure temperature calculated using lattice strain models.

[b] Closure temperature for Pb diffusion in chondrule pyroxenes estimated by Amelin et al. (2005). Age data by Blinova et al. (2007) for Estacado and Mt. Browne, Amelin et al. (2005) for Richardton, and Bouvier et al. (2007) for Nadiabondi and Kernouvé.

[c] Data from Zinner and Göpel (2002). Activation energy and frequency factor by LaTourette and Wasserburg (1998): $E = 274$ kJ/mol, $D_0 = 1.2 \times 10^{-6}$. Closure temperature calculated according to Dodson (1973) at 1000 K/Ma cooling rate and 2 $\mu$m feldspar grain size.

[d] Closure temperature by Cherniak et al. (1991), phosphate U–Pb–Pb age data by Göpel et al. (1994), and Blinova et al. (2007) for Estacado and Mt. Browne.

[e] Ar–Ar ages by Trieloff et al. (2003) and Schwarz et al. (2006) for Mt. Browne, recalculated for miscalibration of K decay constant (Renne et al., 2011; Schwarz et al., 2011, 2012, see text). Closure temperature by Trieloff et al. (2003) and Pellas et al. (1997).

[f] Calculated age at 390 K from time interval between Pu-fission track retention in merrillite at 390 K and Pu-fission track retention by pyroxene at 550 K (corresponds to Ar–Ar feldspar age at 550 K). Data by Trieloff et al. (2003), closure temperature by Pellas et al. (1997).

# Thermal model of the H chondrite parent body constrained by radioisotopic ages (Henke et al. 2012a,b, 2013)

**Optimum model: fitting time temperature curves defined by radioisotopic cooling ages (least square fits)**

**→ Variation layering depth for a specific H chondrite**

**→ Variation of parameter set within reasonable values**

Henke et al. (2013) Icarus 226, 212

Parameter range for the meteoritic parent bodies.

| Quantity | Value | Unit |
|---|---|---|
| Formation time, $t_{form}$ | 1.5–3 | Ma |
| Radius, $R$ | 50–200 | km |
| $^{60}Fe/^{56}Fe$ ratio | $0–2.0 \times 10^{-6}$ | |
| Surface temperature, $T_{srf}$ | 150–400 | K |
| Surface porosity, $\phi_{srf}$ | 0.2–0.8 | |
| bulk heat conductivity, $K_0$ | 1.0–7.0 | W/mK |

# Thermal model of the H chondrite parent body constrained by radioisotopic ages (Henke et al. 2012a,b, 2013)

Optimum model: fitting time temperature curves defined by radioisotopic cooling ages (least square fits)

→ Variation layering depth for a specific H chondrite

→ Variation of parameter set within reasonable values

→ Parameter variation: „Evolution algorithm“ (Rechenberg 1973, 1989; Charbonneau 1995)

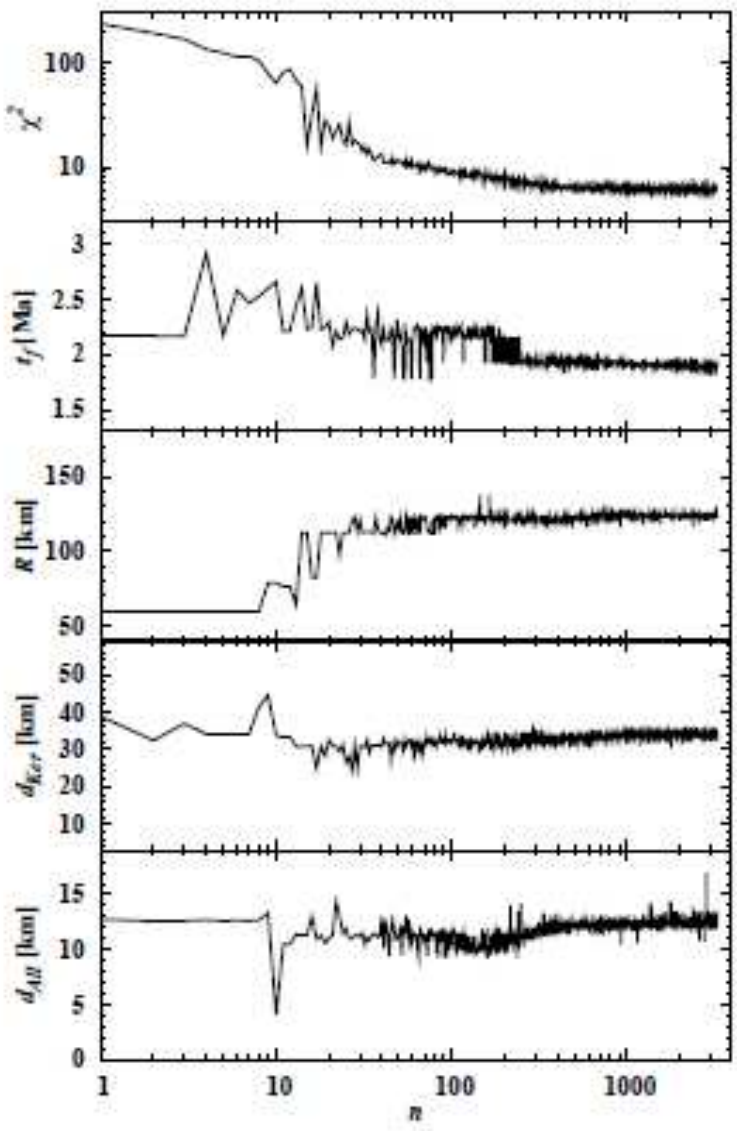


Henke et al. (2012) A&A 545, A135

# Thermal model of the H chondrite parent body constrained by radioisotopic ages
## (Henke et al. 2012a,b, 2013)

**Best fit:**

**Formation time:**
**2.0 Ma after CAIs**

**$^{60}Fe/^{56}Fe=1.4 \times 10^{-8}$**

**Tang & Dauphas 2012:**
**$^{60}Fe/^{56}Fe = (1.08+-0.21) \times 10^{-8}$**
**→ Negligible heating effect by $^{60}Fe$**

**Surface porosity 20%**
**(Porous layer <1km)**

**Fit quality given by $\chi^2$**

| Quantity | | Model |
|---|---|---|
| | | 1 |
| Formation time | $t_{form}$ | 2.026 |
| Radius | $R$ | 189.6 |
| $^{60}Fe/^{56}Fe$ ratio | | 1.43 |
| Surface porosity | $\phi_{srf}$ | 20.1 |
| Surface temperature | $T_{srf}$ | 193 |
| Heat conductivity | $K_b$ | 4.1 |
| Model quality | $\chi^2$ | 6.9338 |
| Maximum temperature | $T_d$ | 1239 |

Henke et al. (2013) Icarus 226, 212

| Meteorite | Type | Depth (km) | $T_{max}$ (K) |
|---|---|---|---|
| Estacado | H6 | 43.6 | 1177 |
| Guarena | H6 | 43.6 | 1177 |
| Kernouvé | H6 | 36.5 | 1172 |
| Mt. Browne | H6 | 23.2 | 1145 |
| Richardton | H5 | 17.5 | 1113 |
| Allegan | H5 | 14.4 | 1083 |
| Nadiabondi | H5 | 11.8 | 1047 |
| Forest Vale | H4 | 6.11 | 917 |
| Ste. Marguerite | H4 | 3.12 | 805 |

# Thermal model of the H chondrite parent body constrained by radioisotopic ages (Henke et al. 2012a,b, 2013)

Henke et al. (2013) Icarus 226, 212

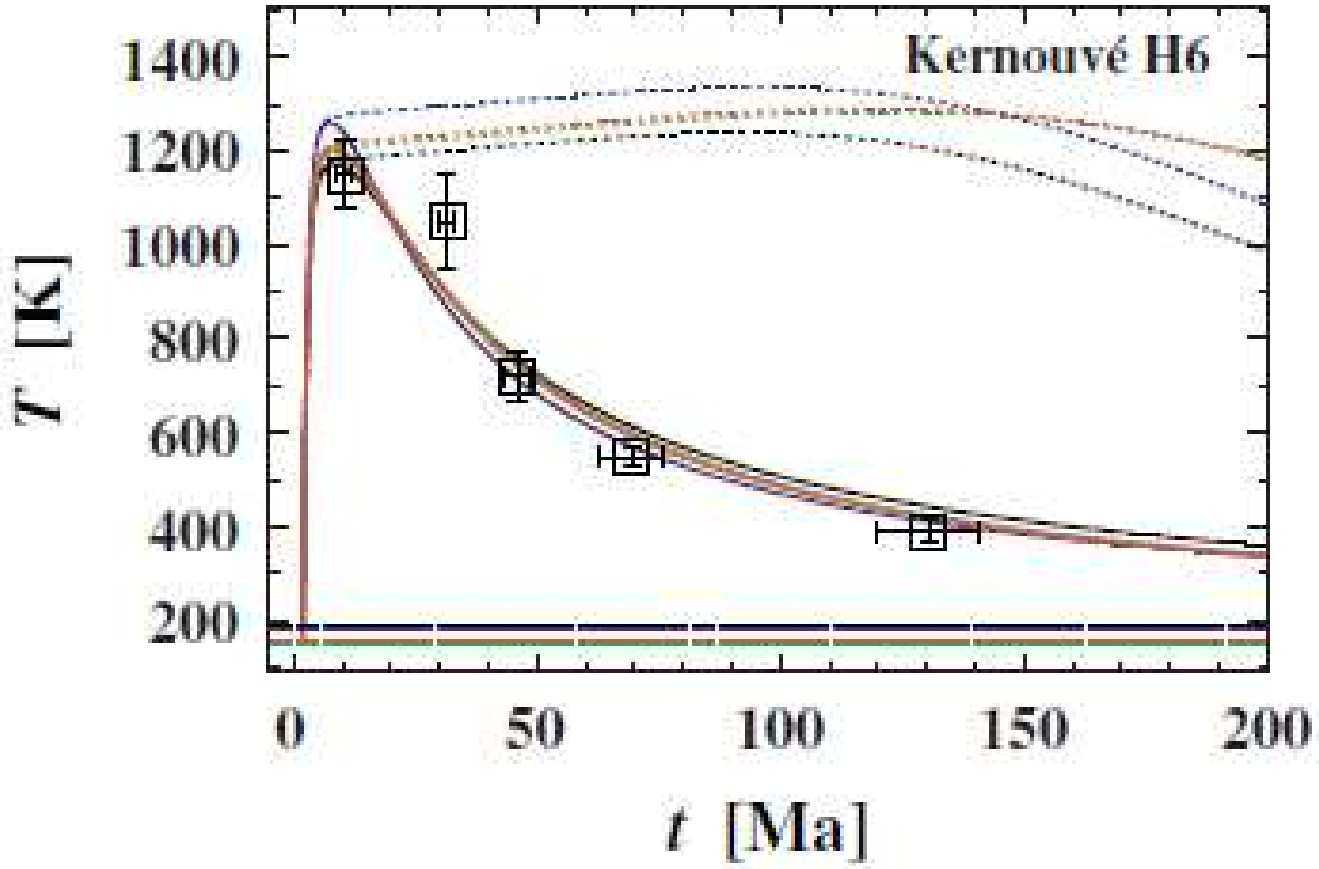

# Thermal model of the H chondrite parent body constrained by radioisotopic ages
## (Henke et al. 2012a,b, 2013)

→ Duration of accretion very likely less than 1 Ma

Henke et al. (2013) Icarus 226, 212

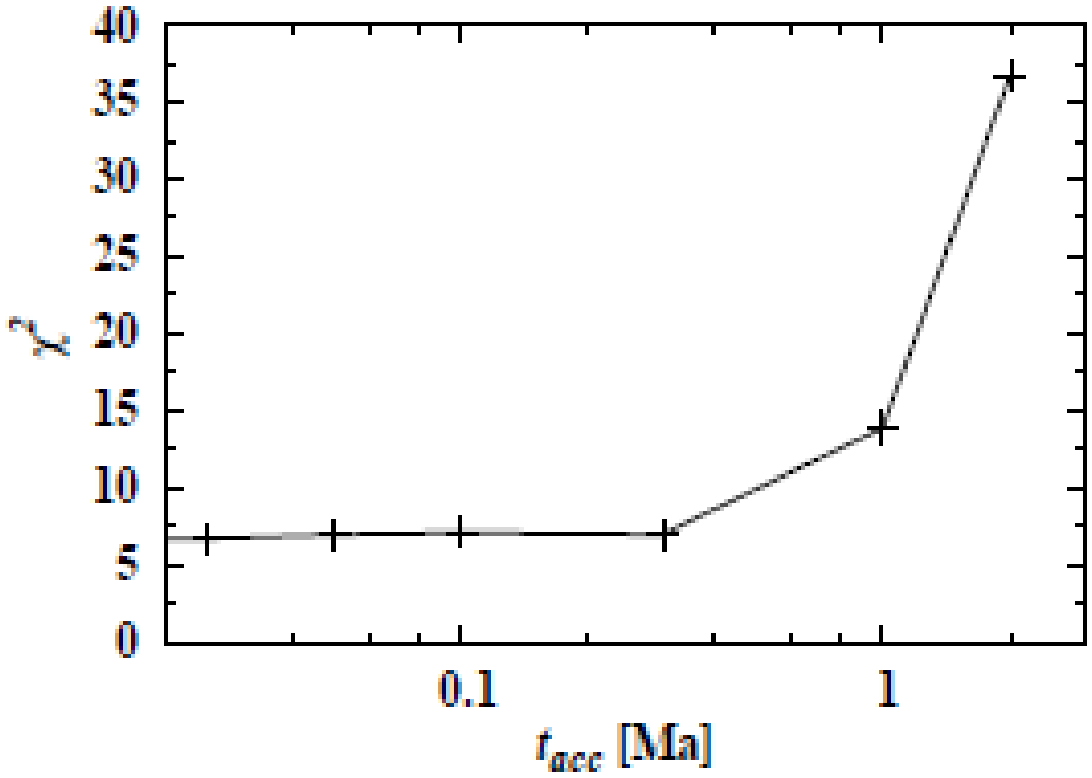

# Modeling the thermal evolution of small bodies

## Melting - differentiation - core formation

Implementation of partial melting of FeNi / FeS and silicates

Melt and heat transport via advection
→ Flow in porous media theory, Darcy flow equation, < 50%melt

Redistribution of radiogenic heat sources:
- lithophile $^{26}$Al partitions into mantle/crust
- siderophile $^{60}$Fe partitions into core

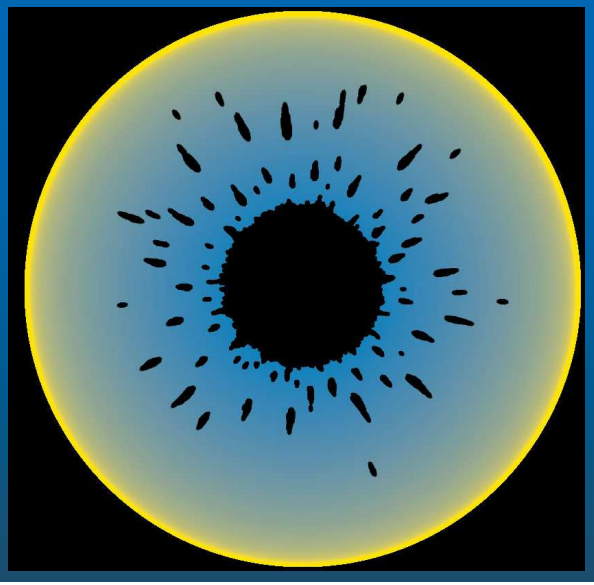

Trieloff & Althaus (2003) Sterne und Weltraum special 2, 83

# Modeling the thermal evolution of small bodies

## Influence of melt and heat transport via porous flow (advection)

## Influence of redistribution of radiogenic heat sources

Neumann et al. (2012) A&A 543, A141

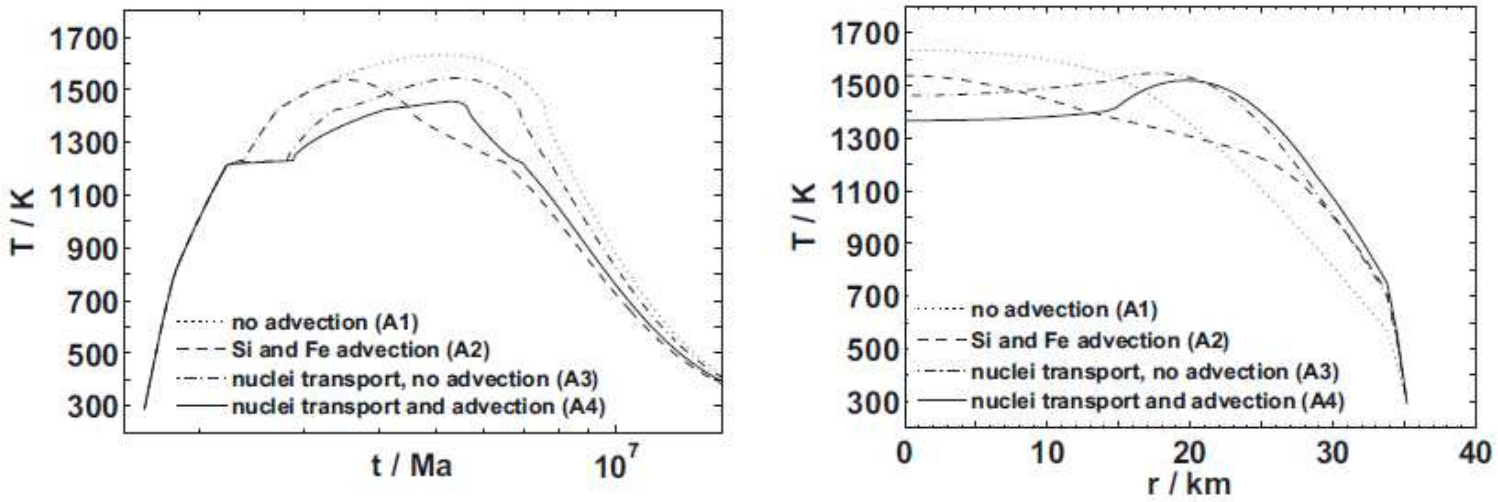


**Fig. 5.** The evolution of the central temperature (*left panel*) and the radial temperature distribution at the instance of the maximum temperature (*right panel*) in a body that accreted instantaneously to $D = 35$ km at $t_0 = 1.6$ Ma. Consideration of both the heat transport by melt and the redistribution of radioactive elements (solid line), consideration of the heat transport by melt and neglection of the redistribution of radioactive elements (dashed line), consideration of the redistribution of radioactive elements and neglection of the heat transport by melt (dot-dashed line), neglection of both the heat transport by melt and the redistribution of radioactive elements (dotted line).

# Modeling the thermal evolution of small bodies

In most models an undifferentiated layer (both sintered and unsintered) remains on top

→ Some chondrite and achondrite classes may originate from the same parent body

Neumann et al. (2012) A&A 543, A141

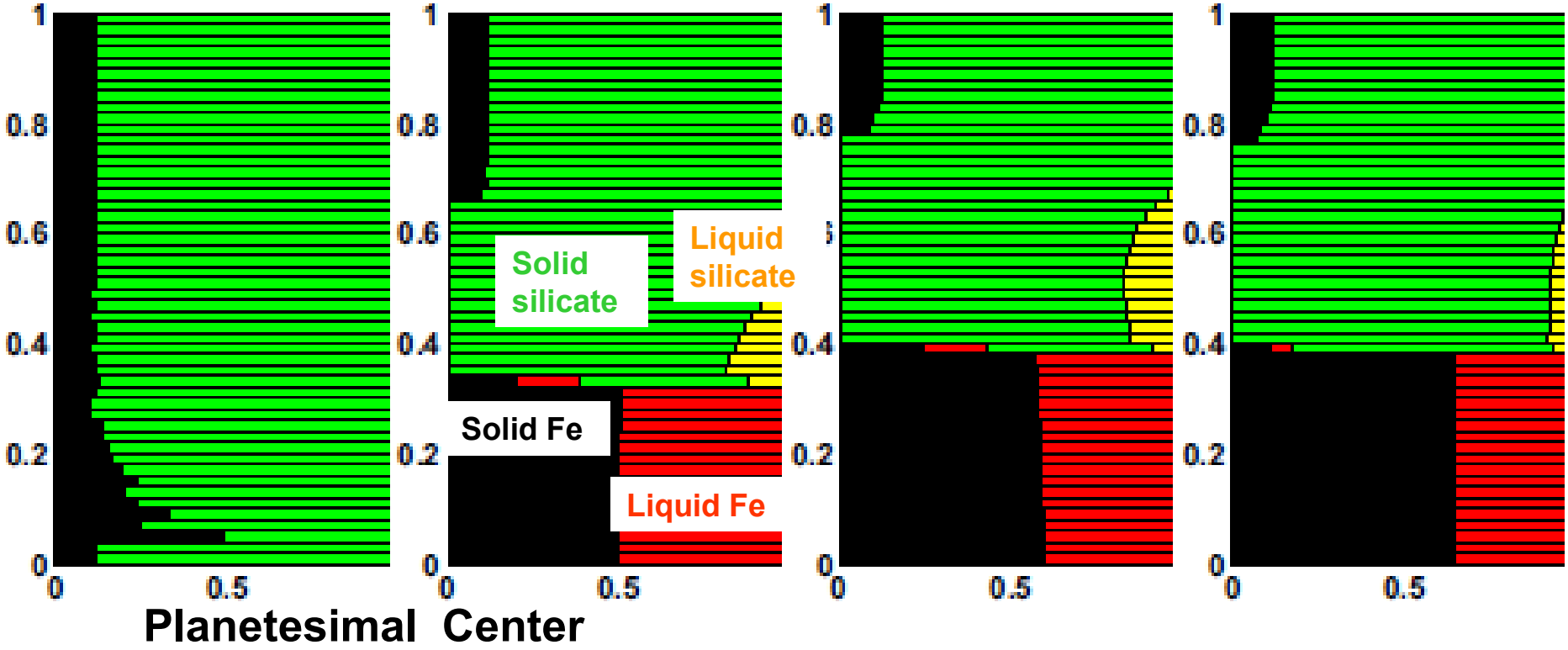

# Summary and conclusions (1)

## Undifferentiated / chondritic bodies:

Improvements by implementation of porosity, cold and hot pressing / sintering in model calculations

Improved sets of experimental data and analyses are available:
→ porosity dependent heat conductivity of micrometer sized silicate aggregates
→ Radioisotopic cooling ages (Hf-W, U-Pb-Pb, Ar-Ar, PU FT)

Best fit model for H chondrite parent body found by „evolution algorithm“:
→ $^{60}Fe/^{56}Fe$ was low ($1.4 \times 10^{-8}$), $^{60}Fe$ did hardly contribute to heating
→ Surface porosity 20% (Porous layer <1 km)
→ Formation time 2.0 Ma after CAIs
→ Accretion was fast (<1 Ma)

Still controversial:
→ Role of impact heating, for some bodies onion shell structure could have been disturbed by early large impacts
→ Distribution of $^{26}Al$

# Summary and conclusions (2)

## Differentiated bodies:

Improvements by implementation of partial melting of FeNi / FeS and silicates, melt and heat transport via porous flow, and redistribution of radiogenic heat sources

Differentiation strongly depends on formation time and accretion process

Metal and silicate segregation processes last between 0.4 Ma and 10 Ma

In most models an undifferentiated layer (both sintered and unsintered) remains on top

→ Some chondrite and achondrite classes may originate from the same parent body